IEEJ Journal of Industry Applications
Vol.6 No.4 pp.278–285 DOI: 10.1541/ieejjia.6.278

Paper

Kinematic Control of Redundant Manipulators for Admitting Joint Range of Motion Maximally

Masahide Ito[*a)] Senior Member, Kazuyoshi Kawatsu[**] Non-member
Masaaki Shibata[***] Senior Member

(Manuscript received Sep. 15, 2016, revised Jan. 30, 2017)

This paper addresses the joint limit avoidance problem in kinematic control of redundant manipulators. A kinematically redundant manipulator has more Degrees of Freedom (DOFs) than are required to perform a given task. An inverse kinematic problem for such a manipulator admits an infinite number of solutions. In its kinematic control, by utilizing the redundant DOFs of the solutions, we can compose a primary task in consideration of a constraint condition. We usually select one of the solutions by introducing a Performance Criterion Function (PCF). The PCF performs a secondary task that has no effect on a primary task. Thus, we can introduce, *e.g.*, joint limit avoidance as a secondary task to the design of a PCF. However, it is hard to perform joint limit avoidance in the case where a joint behaves in the close vicinity of the limit. In this paper, we propose a new PCF for avoiding joint limits. The main feature of the function is to admit the joint range of motion maximally. We adopt the proposed function in the gradient projection method to obtain the redundancy resolution. The effectiveness of the function is demonstrated by both numerical and experimental results. The differences among the proposed and conventional functions are also discussed.

Keywords: kinematically redundant manipulators, joint limits, inverse kinematics, redundancy resolution, kinematic control

1. Introduction

Almost all robotic systems are practically subject to some physical constraints such as actuator saturation, joint limits, and task feasible region. If the constraints are not considered in designing a controller, it can deteriorate performance of the control system drastically and, at worst, lead to instability and breakdown of the system. Thus, it is inherently important to consider the constraints of practical robotic systems.

A manipulator with more Degrees of Freedom (DOFs) than are required to perform a given task, *e.g.*, at the end-effector, is called a (kinematically) redundant manipulator. The redundant manipulator is a control object that it is relatively easy to consider the constraints in its control. The redundant DOFs provide the task execution with flexibility and adaptability. We can obtain a joint motion from a task motion by solving the so-called inverse kinematic problem. However, the problem for a redundant manipulator admits an infinite number of solutions. In Ref. (1), the redundant DOFs in the solutions have been resolved by the *Gradient Projection Method (GPM)* [(2)] so as to maximize a given Performance Criterion Function (PCF), which means that the secondary task is executed according to the PCF. The secondary task has no effect on a primary task, because the secondary task is executed in the null space of the primary task. We can build a desired secondary task which satisfies a constraint condition into a PCF. The secondary task which has performed so far is to avoid obstacles [(3)(4)], kinematic singularities [(5)–(7)], and joint limits [(1)(7)–(16)], to improve the manipulability [(17)], to minimize each joint torque [(18)–(20)], etc.

This paper focuses on avoiding joint limits as the secondary task. By surveying the literature related to this problem, we can classify the conventional PCFs into the following two groups on the basis of their profiles:

a) a function whose profile is convex upward within joint range of motion and which has discontinuity at each joint limit,

b) another function whose profile is approximately convex upward but which is almost flat within joint range of motion and also is continuous even at joint limits[†].

The former is negative concept because we cannot utilize the joint range of motion effectively. The latter has potential to exceed joint limits essentially, *i.e.*, does not work as hard limits at all. In the near future, many robots will be introduced into human-centered environments. For such robots, more dynamic, flexible and complex motion would be required, and also we need to construct a framework so as to hold physical constraints for joints and so as to move joints effectively.

In this paper we propose a new PCF for avoiding joint

a) Correspondence to: Masahide Ito. E-mail: masa-ito@ist.aichi-pu.ac.jp
* School of Information Science and Technology, Aichi Prefectural University
1522-3, Ibaragabasama, Nagakute, Aichi 480-1198, Japan
** Department of Electrical and Mechanical Engineering, Seikei University
3-3-1, Kichijoji-kitamachi, Musashino, Tokyo 180-8633, Japan
*** Department of System Design Engineering, Seikei University
3-3-1, Kichijoji-kitamachi, Musashino, Tokyo 180-8633, Japan

† To put it another way, the whole profile looks like the vertical section view of an upside-down "pan".

limits of redundant manipulators. The main feature of this function is to admit the joint range of motion maximally. We show the specification and one concrete candidate of the PCF. The differences among the proposed and conventional functions are moreover discussed from the viewpoint of the definition. We adopt the proposed function into the GPM to obtain the redundancy resolution. The effectiveness of the function is shown through an example that a three-DOF planar manipulator performs a two-DOF end-effector task. The performance of the proposed method is evaluated in comparison with the conventional ones. A preliminary version of this paper was presented in Refs. (21) and (22). Also, their application to visual servoing was presented in Refs. (23) and (24).

The rest of the paper is organized as follows. Section 2 recalls the inverse kinematics of redundant manipulators and one of the solutions, the GPM. In Sect. 3, a new PCF for the redundancy resolution is presented. In Sects. 4 and 5, we provide numerical and experimental results. Finally, in Sect. 6, the main contributions and the future works of the paper are summarized.

2. Preliminaries

In this paper, we consider the case where an n-DOF manipulator with n actuated (active) joints executes an m ($< n$)-DOF primary task. This section briefly recalls the inverse kinematics of redundant manipulators and one of the solutions, the GPM [1]. We also survey the related works for avoiding joint limits in this framework.

2.1 Inverse Kinematics of Redundant Manipulators

Let $\boldsymbol{q} \in \mathbb{R}^n$ and $\boldsymbol{r} \in \mathbb{R}^m$ be the joint vector and the task vector, respectively. From the geometric relationship, the both are related as follows:

$$\boldsymbol{r} = \boldsymbol{h}(\boldsymbol{q}). \cdots (1)$$

Differentiating Eq. (1) with respect to time gives the forward kinematics

$$\dot{\boldsymbol{r}} = \frac{\partial \boldsymbol{h}}{\partial \boldsymbol{q}}\dot{\boldsymbol{q}} = \boldsymbol{J}(\boldsymbol{q})\dot{\boldsymbol{q}}. \cdots (2)$$

The matrix $\boldsymbol{J} \in \mathbb{R}^{m\times n}$ is the so-called *task Jacobian matrix*.

The inverse kinematics is to solve Eq. (2) with respect to $\dot{\boldsymbol{q}}$. Here we cannot use the inverse of $\boldsymbol{J}$ because $\boldsymbol{J}$ is not square. Usually, regarding the inverse kinematics as to solve

$$\min_{\dot{\boldsymbol{q}}} \|\dot{\boldsymbol{r}} - \boldsymbol{J}(\boldsymbol{q})\dot{\boldsymbol{q}}\|, \cdots (3)$$

we obtain the general solution

$$\dot{\boldsymbol{q}} = \boldsymbol{J}^+(\boldsymbol{q})\,\dot{\boldsymbol{r}} + \boldsymbol{J}^\perp(\boldsymbol{q})\,\boldsymbol{\phi}, \cdots (4)$$

where $\boldsymbol{J}^+ = \boldsymbol{J}^\top(\boldsymbol{J}\boldsymbol{J}^\top)^{-1} \in \mathbb{R}^{n\times m}$ denotes the pseudo-inverse of $\boldsymbol{J}$, $\boldsymbol{J}^\perp = \boldsymbol{I}_n - \boldsymbol{J}^+\boldsymbol{J} \in \mathbb{R}^{n\times n}$ is the orthogonal projection operator into the null-space of $\boldsymbol{J}$, *i.e.*, $\ker \boldsymbol{J}$, and $\boldsymbol{\phi} \in \mathbb{R}^n$ is an arbitrary vector. There exists an infinite number of solutions in Eq. (4) for arbitrary $\boldsymbol{\phi}$. Note that a solution $\dot{\boldsymbol{q}}$ which satisfies $\min_{\dot{\boldsymbol{q}}} \|\dot{\boldsymbol{q}}\|$ in addition to Eq. (3) is equal to the one that $\boldsymbol{\phi} = \boldsymbol{0}_n$ in Eq. (4).

2.2 Gradient Projection Method

The solution $\dot{\boldsymbol{q}}$ in Eq. (4) has redundancy, so we need to resolve it. Liégeois [1] has proposed a redundancy resolution scheme so as to maximize a given PCF using the GPM [2]. This scheme gives the solution

$$\dot{\boldsymbol{q}} = \boldsymbol{J}^+(\boldsymbol{q})\,\dot{\boldsymbol{r}} + k_r\boldsymbol{J}^\perp(\boldsymbol{q})\left(\frac{\partial V}{\partial \boldsymbol{q}}\right)^\top, \cdots (5)$$

where V is a PCF and $k_r (> 0)$ is a scalar parameter[†]. This equation is equal to Eq. (4) with the $\boldsymbol{\phi} = k_r(\partial V/\partial \boldsymbol{q})^\top$.

Now we supposes that the primary task is to track a desired trajectory $\boldsymbol{r}^d$ and the secondary one is to avoid joint limits. Then, on the basis of Eq. (5), a desired joint velocity $\dot{\boldsymbol{q}}^d$ is described as

$$\dot{\boldsymbol{q}}^d = \boldsymbol{J}^+(\boldsymbol{q})\,\dot{\boldsymbol{r}}^d + \boldsymbol{J}^\perp(\boldsymbol{q})\left(\frac{\partial V}{\partial \boldsymbol{q}}\right)^\top. \cdots (6)$$

Note that Eq. (6) includes k_r in V for the sake of the following discussion. We need to select V appropriately so as to achieve joint limit avoidance as the secondary task.

2.3 Related Works for Avoiding Joint Limits

We have surveyed the related works which treat joint limit avoidance as the secondary task. As a result, PCFs V which have been proposed for avoiding joint limits [1][7]–[16][27] are roughly classified into the following four typical types[††]:

1) **Liégeois-type function** To the authors' knowledge, a PCF for avoiding joint limits was first proposed by Liégeois [1]. The Liégeois's function is described as

$$V(\boldsymbol{q}) = -k_r \sum_{i=1}^{n}\left(\frac{q_i - q_i^{\mathrm{mid}}}{\Delta q_i}\right)^2, \cdots (7)$$

where $q_i^{\max}$, $q_i^{\min}$ are the upper and lower limits of the i-th joint, $q_i^{\mathrm{mid}} := (q_i^{\max} + q_i^{\min})/2$, and $\Delta q_i := q_i^{\max} - q_i^{\min}$, respectively.

2) **Tsai-type function** Tsai [9] proposed the following PCF based on the exponential function:

$$V(\boldsymbol{q}) = 1 - \exp\left(k_r \prod_{i=1}^{n}\frac{(q_i - q_i^{\max})(q_i - q_i^{\min})}{\Delta {q_i}^2}\right). \cdots (8)$$

Nelson *et al.* [7] multiplied this function by the manipulability [17] to implement simultaneous avoidance of joint limits and kinematic singularities in an application to visual servoing.

3) **Zghal-type function** The following PCF was proposed by Zghal, *et al.* [10]:

$$V(\boldsymbol{q}) = -\frac{1}{4}k_r \sum_{i=1}^{n}\frac{\Delta {q_i}^2}{(q_i - q_i^{\max})(q_i - q_i^{\min})}. \cdots (9)$$

Chan *et al.* [11] introduced the PCF (9) not to the GPM but

[†] When k_r is defined to be a *negative* number, Liégeois's scheme is also regarded as the redundancy resolution to *minimize* a given PCF.

[††] As one of algorithmic approaches in the related studies, the Saturation in the Null Space (SNS) method was recently proposed by Flacco, *et al.* [25]. We here do not include the SNS method in the classification of the conventional PCFs, because this method does not use an explicit PCF. In the SNS method, solving a quadratic programming problem numerically under hard joint constraints that may saturate during motion achieves joint limit avoidance.

to the *Weighted Least-Norm (WLN) solution*[26]. Also, an algorithm proposed in Ref. (11) allows the weighted matrix not to be constant but to be switched according to the variation of the gradient of the PCF. Recently, Atawnih, *et al.*[27] applied the prescribed performance control method[28] to controlling redundant robots in order to achieve joint limit avoidance. In its design, the following natural logarithmic function is used:

$$V(\boldsymbol{q}) = -\frac{1}{2}k_r \sum_{i=1}^{n} \ln^2 \frac{1 + \frac{q_i - q_i^{\mathrm{mid}}}{b_i}}{1 - \frac{q_i - q_i^{\mathrm{mid}}}{b_i}},$$

where $b_i := \Delta q_i/2$. This PCF is defined only within joint range of motion, but has common features with Eq. (9), which is therefore categorized as the Zghal-type function.

4) **Marchand-type function** Marchand, *et al.*[12] proposed the following switched PCF:

$$V(\boldsymbol{q}) = \begin{cases} -\frac{1}{2}k_r \sum_{i=1}^{n} \frac{(q_i - \bar{q}_i^{\max})^2}{\Delta q_i}, & \text{if } q_i > \bar{q}_i^{\max} \\ -\frac{1}{2}k_r \sum_{i=1}^{n} \frac{(q_i - \bar{q}_i^{\min})^2}{\Delta q_i}, & \text{if } q_i < \bar{q}_i^{\min} \\ 0, & \text{otherwise,} \end{cases} \quad \cdots\cdots\cdots\cdots\cdots (10)$$

where $\bar{q}_i^{\max} := q_i^{\max} - \rho\Delta q_i$, $\bar{q}_i^{\min} := q_i^{\min} + \rho\Delta q_i$, $\rho \in (0, 1/2)$. Chaumette *et al.*[13] pointed out some problems on k_r usually determined by trial and error, and proposed an iterative solution instead of the GPM. Mansard *et al.*[14] also proposed a solution that increases DOFs of the secondary task to improve control performance for achieving the task. Moreover, Marey *et al.*[15][16] proposed a new large projection operator by defining the primary task as the norm of the total error, and developed a switching strategy and an adaptive gain function to give an adequate solution. The solutions exploit the PCF (10) to implement joint limit avoidance in an application to visual servoing.

The profiles of the four PCFs on q_i are shown in Fig. 1. The value of each k_r is appropriately selected so as to be comparable with the four functions. We can find the following features from each definition and Fig. 1:

- Every PCF except the Marchand-type function is convex upward, which has its maximal value at the midpoint in joint range of motion.
- Every PCF except the Zghal-type function is continuous on joint limits.

The former feature means that a joint variable converges to the midpoint in joint range of motion. A PCF which has such feature is expected to avoid joint limits, but it is negative concept because we cannot exploit the joint range of motion effectively. The latter feature indicates that a joint variable potentially exceeds its limit depending on the selection of k_r, the desired joint trajectories which achieve the primary task, and so on.

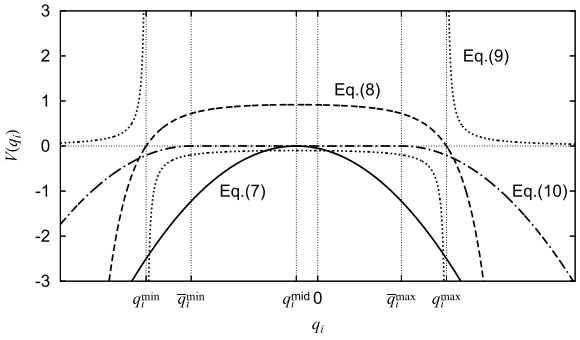

Fig. 1. Profiles of the conventional PCFs: solid, broken, dotted, and chain lines denote Eq. (7) with $k_r = 10$, Eq. (8) with $k_r = 10$, Eq. (9) with $k_r = 0.1$, and Eq. (10) with $k_r = 10$, $\rho = 0.15$, respectively

3. Maximal Admission of Joint Range of Motion

As stated in Sect. 2.3, joint limit avoidance using the conventional PCF may be negatively achieved or may fail. So, it is difficult to achieve joint limit avoidance, *e.g.*, in the case where a joint variable behaves in the close vicinity of the limit. In this section a new PCF for avoiding joint limits is proposed. We show the definition and one concrete candidate. We also compare the proposed and conventional functions from the viewpoint of their definitions.

3.1 Performance Criterion Function for Admitting Joint Range of Motion Maximally Supposing a challenging situation that can be hard for the conventional functions to treat, we give an original concept for the joint limit avoidance problem. The concept is to avoid joint limits strictly and to utilize the joint range of motion maximally. Let us call this concept *maximal admission of joint range of motion*. The conditions that a PCF for admitting the joint range of motion maximally, $V(\boldsymbol{q}) = k_r \sum_{i=1}^{n} V_i(q_i)$, should satisfy are defined as follows:

i) Let $\mathcal{N}_i^{\max} := \{ q_i \mid \bar{q}_i^{\max} \le q_i < q_i^{\max} \}$ and $\mathcal{N}_i^{\min} := \{ q_i \mid q_i^{\min} < q_i \le \bar{q}_i^{\min} \}$, where $q_i^{\max}$ and $q_i^{\min}$ are the upper and lower limits on the i-th joint, $\bar{q}_i^{\max} := q_i^{\max} - \rho\Delta q_i$, $\bar{q}_i^{\min} := q_i^{\min} + \rho\Delta q_i$, $\rho \in (0, 1/2)$, and $\Delta q_i := q_i^{\max} - q_i^{\min}$, respectively. Function $V_i(q_i)$ satisfies

$$\frac{\mathrm{d}V_i}{\mathrm{d}q_i} \to \begin{cases} -\infty & \text{as } q_i \to q_i^{\max} - 0 \\ 0 & \text{as } q_i \to \bar{q}_i^{\max} + 0 \end{cases}, \quad \text{for } q_i \in \mathcal{N}_i^{\max}$$

and

$$\frac{\mathrm{d}V_i}{\mathrm{d}q_i} \to \begin{cases} 0 & \text{as } q_i \to \bar{q}_i^{\min} - 0 \\ +\infty & \text{as } q_i \to q_i^{\min} + 0 \end{cases}, \quad \text{for } q_i \in \mathcal{N}_i^{\min}.$$

ii) Let $\mathcal{M}_i := \{ q_i \mid q_i^{\min} < q_i < q_i^{\max} \}$. For $q_i \in \mathcal{M}_i - (\mathcal{N}_i^{\max} + \mathcal{N}_i^{\min})$, function $V_i(q_i)$ satisfies $\partial V_i/\partial q_i = 0$.

Figure 2 shows the schematic representation of an ideal PCF which satisfy both Conditions i) and ii). We introduce the region for avoiding joint limits at the neighborhood of the limits in the same way as in Ref. (12). Condition i) means avoiding each joint limit only in the region. On the other hand, Condition ii) means performing only the primary task (*i.e.*, doing nothing as the secondary task) everywhere except in the region.

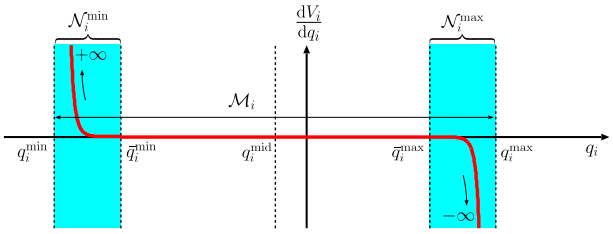

Fig. 2. Gradient profile of an ideal PCF

Liégeois-type function (7) and Tsai-type function (8) satisfy neither Condition i) nor ii). The Zghal-type function (9) satisfies Condition i) but does not satisfy Condition ii). The Marchand-type function (10) does not satisfy Condition i) but satisfies Condition ii). Accordingly, all the conventional PCFs (7)–(10) do not satisfy both Conditions i) and ii).

3.2 Tangent-based Candidate Condition i) requires an upward-convex function bounded with respect to q_i. Although such a function exists variously, we focus on the boundedness of the tangent function with respect to the domain of definition. We here propose the following tangent-based function as one candidate of PCFs which satisfies the above Conditions i) and ii):

$$V(\boldsymbol{q}) = k_r \sum_{i=1}^{n} V_i(q_i),$$

$$V_i(q_i) = \begin{cases} -\tan^j(\alpha_i(q_i - \bar{q}_i^{\max})), & \text{if } q_i \in \mathcal{N}_i^{\max} \\ -\tan^j(\alpha_i(q_i - \bar{q}_i^{\min})), & \text{if } q_i \in \mathcal{N}_i^{\min} \\ 0, & \text{otherwise} \end{cases}$$

$$(j = 2, 4, 6, \ldots), \quad \cdots\cdots\cdots\cdots\cdots\cdots\cdots\cdots\cdots\cdots (11)$$

where $\alpha_i := \pi/(2\rho\Delta q_i)$, k_r and ρ are two tuning parameters. This function is designed by splitting a tangent function raised to the even-number-th power into two parts horizontally and then inserting a line segment between them so as to reconnect them. Differentiating Eq. (11) with respect to q_i, the gradient vector is derived as follows:

$$\frac{\partial V}{\partial \boldsymbol{q}} = \begin{bmatrix} \dfrac{\partial V}{\partial q_1} & \cdots & \dfrac{\partial V}{\partial q_n} \end{bmatrix} = \begin{bmatrix} \dfrac{\mathrm{d}V}{\mathrm{d}q_1} & \cdots & \dfrac{\mathrm{d}V}{\mathrm{d}q_n} \end{bmatrix},$$

$$\frac{\mathrm{d}V_i}{\mathrm{d}q_i} = \begin{cases} -\dfrac{jk_r\alpha_i\tan^{j-1}(\alpha_i(q_i - \bar{q}_i^{\max}))}{\cos^2(\alpha_i(q_i - \bar{q}_i^{\max}))}, & \text{if } q_i \in \mathcal{N}_i^{\max} \\ -\dfrac{jk_r\alpha_i\tan^{j-1}(\alpha_i(q_i - \bar{q}_i^{\min}))}{\cos^2(\alpha_i(q_i - \bar{q}_i^{\min}))}, & \text{if } q_i \in \mathcal{N}_i^{\min} \\ 0, & \text{otherwise.} \end{cases}$$

$$\cdots\cdots\cdots\cdots\cdots\cdots (12)$$

The profiles of the proposed function and its gradient are depicted in Fig. 3. Using $\alpha(q_i - \bar{q}_i^{\max}) = \pi(q_i - \bar{q}_i^{\max})/(2\rho\Delta q_i) \to \pi/2$ as $q_i \to q_i^{\max} - 0$ and $\alpha(q_i - \bar{q}_i^{\min}) = \pi(q_i - \bar{q}_i^{\min})/(2\rho\Delta q_i) \to -\pi/2$ as $q_i \to q_i^{\min} + 0$, it follows from Eq. (12) that $\lim_{q_i \to q_i^{\max} - 0} \mathrm{d}V_i/\mathrm{d}q_i = -\infty$, $\lim_{q_i \to \bar{q}_i^{\max} + 0} \mathrm{d}V_i/\mathrm{d}q_i = \lim_{q_i \to \bar{q}_i^{\min} - 0} \mathrm{d}V_i/\mathrm{d}q_i = 0$, and $\lim_{q_i \to q_i^{\min} + 0} \mathrm{d}V_i/\mathrm{d}q_i = \infty$. So, it is certain that the gradient (12) satisfies both Conditions i) and ii).

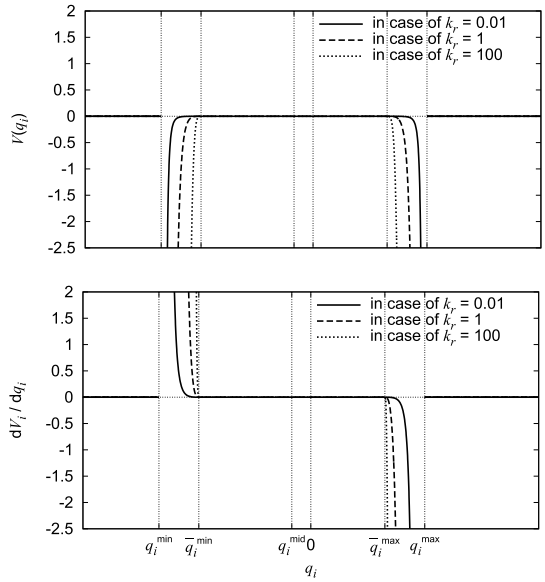

Fig. 3. Profiles of the tangent-based PCF ($j = 4$)

Remark 1 *Differentiating each element of the gradient vector* (12) *with respect to* q_i*, we obtain Eq.* (13)*. When* $j = 2$*, it follows from Eq.* (13) *that* $\lim_{q_i \to \bar{q}_i^{\max} + 0} \mathrm{d}^2 V_i/\mathrm{d}q_i^2 = \lim_{q_i \to \bar{q}_i^{\min} - 0} \mathrm{d}^2 V_i/\mathrm{d}q_i^2 = -2k_r\alpha_i^2 \neq 0$*. This means that* $\mathrm{d}^2 V_i/\mathrm{d}q_i^2$ *is discontinuous at* $q_i = \bar{q}_i^{\max}, \bar{q}_i^{\min}$ *in* $\mathcal{M}_i$*, i.e.,* $\mathrm{d}V_i/\mathrm{d}q_i$ *is a* C^0*-function in* $\mathcal{M}_i$*, as shown in Fig. 4(a). On the other hand, when* $j = 4, 6, \ldots$*, it follows from Eq.* (13) *that* $\lim_{q_i \to \bar{q}_i^{\max} + 0} \mathrm{d}^2 V_i/\mathrm{d}q_i^2 = 0$ *and* $\lim_{q_i \to \bar{q}_i^{\min} - 0} \mathrm{d}^2 V_i/\mathrm{d}q_i^2 = 0$*. This means that* $\mathrm{d}^2 V_i/\mathrm{d}q_i^2$ *is continuous in* $\mathcal{M}_i$*, i.e.,* $\mathrm{d}V_i/\mathrm{d}q_i$ *is a* C^1*-function in* $\mathcal{M}_i$*, as shown in Fig. 4(b), (c).* ◁

In this paper we adopt the proposed tangent-based function (11) in Eq. (6) based on the GPM. Consequently, we obtain a desired joint velocity trajectory $\dot{\boldsymbol{q}}^d$ so as to achieve simultaneously tracking a desired trajectory $\dot{\boldsymbol{r}}^d$ as the primary task and admitting the joint range of motion maximally as the secondary task. The desired joint trajectory $\boldsymbol{q}^d$ is calculated by a step-by-step integration of $\dot{\boldsymbol{q}}^d$, such as the Euler method and the Runge-Kutta method. Note that the proposed tangent-based function can also adopt the other solution, *e.g.*,

$$\frac{\partial^2 V}{\partial q_i^2} = \frac{\mathrm{d}^2 V_i}{\mathrm{d}q_i^2} = \begin{cases} -\dfrac{2k_r\alpha_i^2\tan^{j-2}(\alpha_i(q_i - \bar{q}_i^{\max}))}{\cos^4(\alpha_i(q_i - \bar{q}_i^{\max}))}\{j - 1 + 2\sin^2(\alpha_i(q_i - \bar{q}_i^{\max}))\}, & \text{if } q_i \in \mathcal{N}_i^{\max} \\ -\dfrac{2k_r\alpha_i^2\tan^{j-2}(\alpha_i(q_i - \bar{q}_i^{\min}))}{\cos^4(\alpha_i(q_i - \bar{q}_i^{\min}))}\{j - 1 + 2\sin^2(\alpha_i(q_i - \bar{q}_i^{\min}))\}, & \text{if } q_i \in \mathcal{N}_i^{\min} \\ 0, & \text{otherwise} \end{cases} \quad (j = 2, 4, 6, \ldots)$$

$$\cdots\cdots\cdots\cdots\cdots\cdots\cdots\cdots\cdots\cdots\cdots\cdots\cdots\cdots\cdots\cdots\cdots\cdots\cdots\cdots\cdots\cdots\cdots\cdots\cdots\cdots\cdots\cdots (13)$$

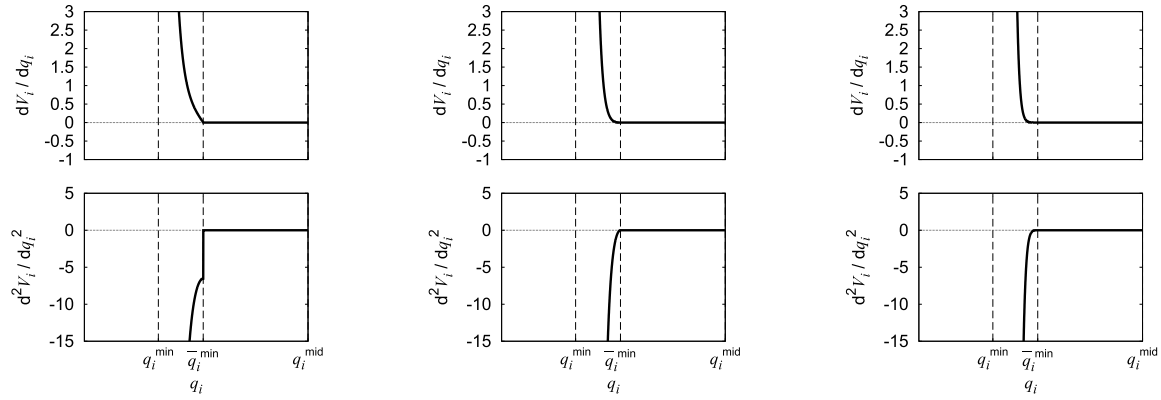

(a) $j = 2$ (b) $j = 4$ (c) $j = 6$

Fig. 4. Gradient profiles of the proposed tangent-based PCF around $q_i = \bar{q}_i^{\min}$

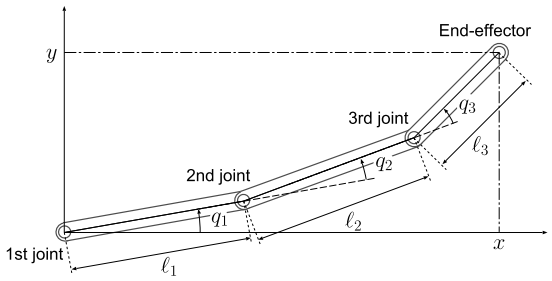

Fig. 5. A three-DOF planar manipulator

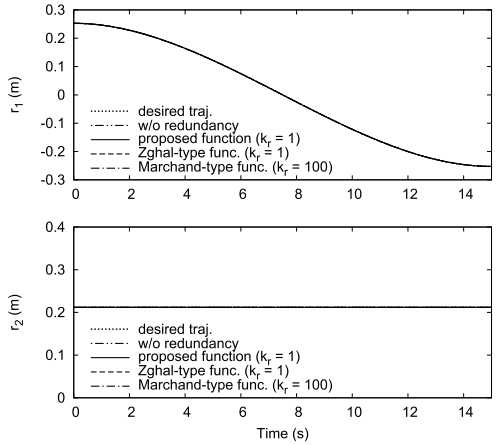

Fig. 6. Simulation results (end-effector position)

the WLN solution [26], the Chaumette *et al.*'s iterative solution [13], the Mansard *et al.*'s solution [14], etc.

In the following two sections, we show the effectiveness of the proposed tangent-based function through a simulation and an experiment.

4. Simulation

This section shows a numerical example to evaluate kinematic control using the proposed tangent-based function. The proposed function is also compared with the conventional functions.

Consider a three-DOF planar manipulator ($n = 3$) depicted in Fig. 5. Each joint is rotational joint actuated by an actuator, such as a DC servo motor. The primary task is to track a desired trajectory at the end-effector ($m = 2$). Let $\boldsymbol{q} := [\, q_1,\ q_2,\ q_3\,]^\top$ and $\boldsymbol{r} = [\, r_1,\ r_2\,]^\top := [\, x,\ y\,]^\top$ be the joint angle vector and the task vector, *i.e.*, the position vector of the end-effector. Then $\boldsymbol{h}$ in Eq. (1) and $\boldsymbol{J}$ in Eq. (2) are

$$\boldsymbol{h}(\boldsymbol{q}) = \begin{bmatrix} \ell_1 \mathrm{C}_1 + \ell_2 \mathrm{C}_{12} + \ell_3 \mathrm{C}_{123} \\ \ell_1 \mathrm{S}_1 + \ell_2 \mathrm{S}_{12} + \ell_3 \mathrm{S}_{123} \end{bmatrix},$$

$$\boldsymbol{J}(\boldsymbol{q}) = \begin{bmatrix} -\ell_1 \mathrm{S}_1 - \ell_2 \mathrm{S}_{12} - \ell_3 \mathrm{S}_{123} & \\ \ell_1 \mathrm{C}_1 + \ell_2 \mathrm{C}_{12} + \ell_3 \mathrm{C}_{123} & \\ & -\ell_2 \mathrm{S}_{12} - \ell_3 \mathrm{S}_{123} \quad -\ell_3 \mathrm{S}_{123} \\ & \ell_2 \mathrm{C}_{12} + \ell_3 \mathrm{C}_{123} \quad \ell_3 \mathrm{C}_{123} \end{bmatrix}, \cdots\cdots\cdots (14)$$

where $\ell_i,\ i = 1, 2, 3$ denotes the length of each link, $\mathrm{S}_{ijk} := \sin(q_i + q_j + q_k)$ and $\mathrm{C}_{ijk} := \cos(q_i + q_j + q_k)$, respectively. Note that the manipulator configures kinematic singularities when $(q_2, q_3) = (\pm\alpha\pi, \pm\beta\pi),\ \forall\alpha, \beta \in \mathbb{Z}$.

We adopt the following third-order time polynomial trajectory as the desired trajectory at the end-effector:

$$\boldsymbol{r}^d(t) = \begin{bmatrix} a_{10} + a_{11}t + a_{12}t^2 + a_{13}t^3 \\ a_{20} + a_{21}t + a_{22}t^2 + a_{23}t^3 \end{bmatrix}, \cdots\cdots\cdots (15)$$

where the coefficients are $a_{i0} = r_i(0)$, $a_{i1} = \dot{r}_i(0)$, $a_{i2} = (1/t_f^2)\{3(r_i(t_f) - r_i(0)) - (2\dot{r}_i(0) + \dot{r}_i(t_f))\, t_f\}$, $a_{i3} = (1/t_f^3)\{-2(r_i(t_f) - r_i(0)) + (\dot{r}_i(t_f) + \dot{r}_i(0))\, t_f\}$, and t_f is the terminal time, respectively. Giving an initial conditions $\boldsymbol{r}(0)$, $\dot{\boldsymbol{r}}(0)$ and a terminal conditions $\boldsymbol{r}(t_f)$, $\dot{\boldsymbol{r}}(t_f)$, the desired trajectory $\boldsymbol{r}^d(t)$ is uniquely determined by Eq. (15). Differentiating Eq. (15) with respect to time, we substitute $\dot{\boldsymbol{r}}^d(t)$ in Eq. (6) with

$$\dot{\boldsymbol{r}}^d(t) = \begin{bmatrix} a_{11} + 2a_{12}t + 3a_{13}t^2 \\ a_{21} + 2a_{22}t + 3a_{23}t^2 \end{bmatrix}. \cdots\cdots\cdots\cdots (16)$$

To concentrate on avoiding joint limits in this paper, we consider only a situation that the manipulator does not configure any kinematic singularities during movement. Let $\boldsymbol{r}(0) \simeq (0.25\,\mathrm{m}, 0.21\,\mathrm{m})$, $\dot{\boldsymbol{r}}(0) = \boldsymbol{0}_2$ and $\boldsymbol{r}(t_f) = (-r_1(0), r_2(0))$, $\dot{\boldsymbol{r}}(t_f) = \dot{\boldsymbol{r}}(0)$, $t_f = 15\,\mathrm{s}$ be the initial and terminal conditions, respectively. The physical and tuning parameters are as follows: $\ell_1 = \ell_2 = 0.2\,\mathrm{m}$, $\ell_3 = 0.047\,\mathrm{m}$, $(\, q_1^{\max},\ q_2^{\max},\ q_3^{\max}\,) = (\, -q_1^{\min},\ -q_2^{\min},\ -q_3^{\min}\,) = (\, 180\,\mathrm{deg},\ 120\,\mathrm{deg},\ 180\,\mathrm{deg}\,)$, and $\rho = 0.1$.

The simulation results are shown in Figs. 6 and 7. For comparison, the results in the case of the Zghal-type and the Marchand-type functions are also included. Each graph shows the case of three kinds of k_r and the case of no

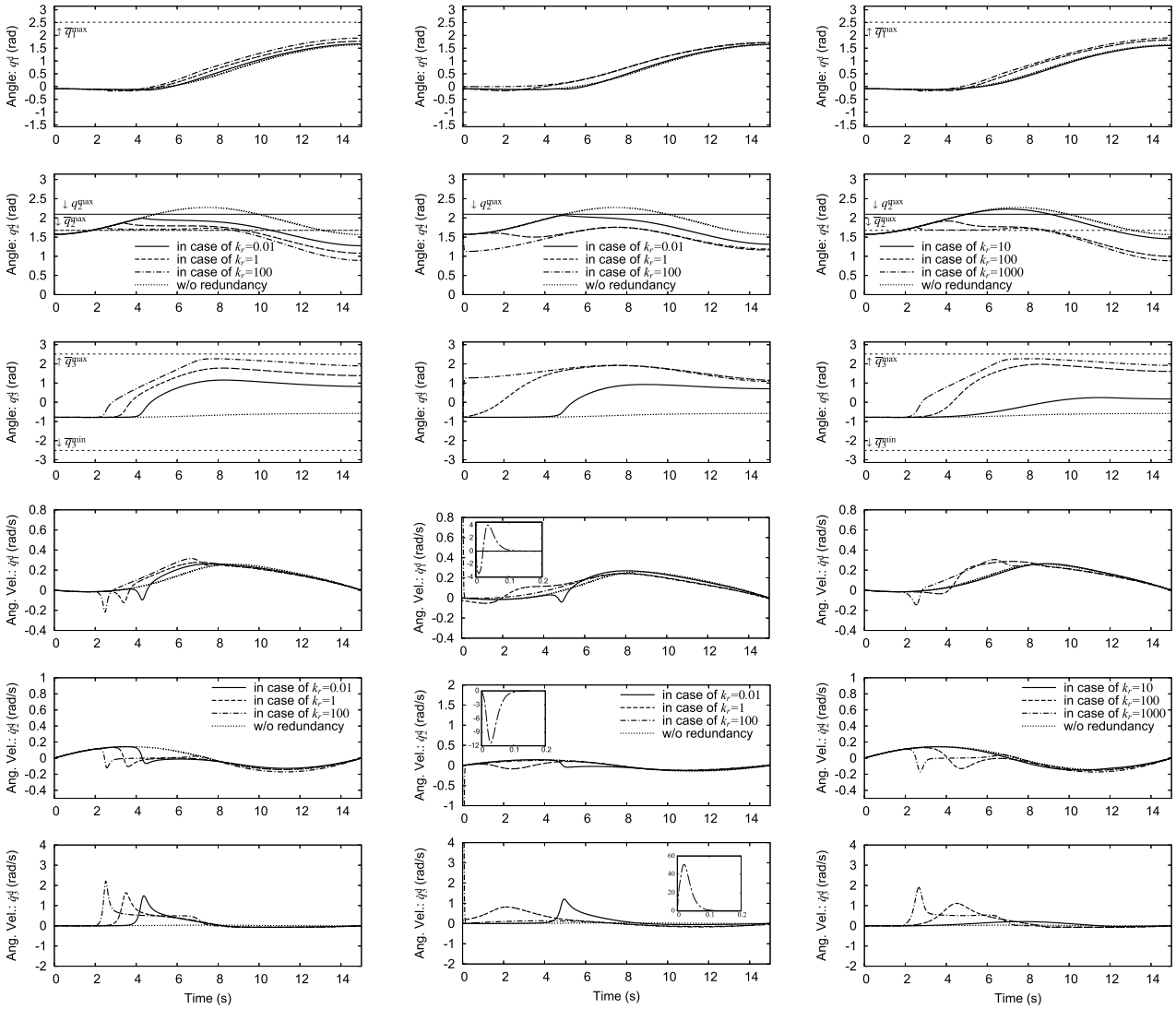

(a) Proposed function (b) Zghal-type function (c) Marchand-type function

Fig. 7. Simulation results (joint angles and angular velocities)

redundancy ($V = 0$). We calculated $\boldsymbol{q}^d(t)$ by using the fourth-order classical Runge-Kutta method.

Figure 6 shows that the primary task was achieved in every case. We also confirmed the same results even when the value of k_r is different from the one in Fig. 6. In the case of the Zghal-type function, joint limit avoidance was succeeded without depending on the value of k_r ($\neq 0$). However the secondary task was executed in all range of motion at each joint and, especially, the desired velocities with steep variation was generated at the beginning of the task. In the case of the Marchand-type function, the second joint angle exceeded its limit depending on the value of k_r. In the case of the proposed tangent-based function, each joint angle avoided its limits without depending on the value of k_r. These results exhibit the effectiveness of the proposed tangent-based function. Note that the avoidance behavior intuitively depends on two parameters k_r and ρ.

5. Experiment

This section provides experimental results to show the practical usefulness of our proposed method. We here adopt a PD feedback control law with disturbance observer [29] so as to perform kinematic control artificially by tracking the trajectory generated in the same way with the previous section. It is well known that the motion control system based on the disturbance observer is robust against system parameter variations and external disturbances [29]. In contrast, the computed torque control method [30] requires accurate parameter identification.

5.1 PD Feedback Control with Disturbance Observer

The dynamics can be modeled as

$$\boldsymbol{M}(\boldsymbol{q})\ddot{\boldsymbol{q}} + \boldsymbol{c}(\boldsymbol{q}, \dot{\boldsymbol{q}}) = \underbrace{\boldsymbol{K}_t \boldsymbol{I}_a}_{\boldsymbol{\tau}_a} - \boldsymbol{\tau}_f + \boldsymbol{\tau}_{\text{ext}}, \cdots\cdots\cdots \quad (17)$$

where $\boldsymbol{q} \in \mathbb{R}^3$ is the joint vector, $\boldsymbol{K}_t = \text{diag}\{K_{t1}, K_{t2}, K_{t3}\}$ is the torque constant matrix, $\boldsymbol{I}_a \in \mathbb{R}^3$ is the armature current vector, $\boldsymbol{\tau}_a$ is the actuator torque, $\boldsymbol{\tau}_f$ is the friction torque, $\boldsymbol{\tau}_{\text{ext}}$ is the external torque, $\boldsymbol{M} \in \mathbb{R}^{3\times 3}$ is the inertia matrix, and $\boldsymbol{c} \in \mathbb{R}^3$ is the Coriolis and centrifugal force vector, respectively. In practice, $\boldsymbol{K}_t$ is not constant but fluctuant. Let $\boldsymbol{K}_t = \bar{\boldsymbol{K}}_t + \Delta\boldsymbol{K}_t$, where $\bar{\boldsymbol{K}}_t$ and $\Delta\boldsymbol{K}_t$ are the nominal and fluctuant parts of $\boldsymbol{K}_t$. Also, we regard $\boldsymbol{M}$ as $\boldsymbol{M}(\boldsymbol{q}) =$

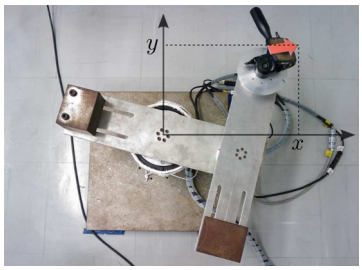

Fig. 8. The experimental setup

$\boldsymbol{M}_d(\boldsymbol{q}) + \boldsymbol{M}_c(\boldsymbol{q})$, where $\boldsymbol{M}_d$ and $\boldsymbol{M}_c$ are the diagonal part and the remainder of $\boldsymbol{M}$. Furthermore, we suppose that $\boldsymbol{M}_d$ is divided into the nominal part $\bar{\boldsymbol{M}}_d$ and the remainder $\Delta\boldsymbol{M}_d$ as $\boldsymbol{M}_d(\boldsymbol{q}) = \bar{\boldsymbol{M}}_d + \Delta\boldsymbol{M}_d(\boldsymbol{q})$. Then, Eq. (17) can be rewritten as $\ddot{\boldsymbol{q}} = \bar{\boldsymbol{M}}_d^{-1}(\bar{\boldsymbol{K}}_t\boldsymbol{I}_a - \boldsymbol{\tau}_{\rm dis})$, where a $\boldsymbol{\tau}_{\rm dis} := \{\Delta\boldsymbol{M}_d(\boldsymbol{q}) + \boldsymbol{M}_c(\boldsymbol{q})\}\ddot{\boldsymbol{q}} + \boldsymbol{c}(\boldsymbol{q},\dot{\boldsymbol{q}}) - \Delta\boldsymbol{K}_t\boldsymbol{I}_a + \boldsymbol{\tau}_f - \boldsymbol{\tau}_{\rm ext}$ as the disturbance torque. To estimate $\boldsymbol{\tau}_{\rm dis}$, we adopt the following disturbance observer[29]: $\hat{\boldsymbol{T}}_{\rm dis}(s) = \boldsymbol{G}_{\rm LP}(s)\{\bar{\boldsymbol{K}}_t\boldsymbol{\mathcal{I}}_a(s) - \bar{\boldsymbol{M}}_d s\cdot s\boldsymbol{Q}(s)\}$, where $\hat{\boldsymbol{T}}_{\rm dis}(s) := \mathcal{L}[\hat{\boldsymbol{\tau}}_{\rm dis}(t)]$, $\boldsymbol{\mathcal{I}}_a(s) := \mathcal{L}[\boldsymbol{I}_a(t)]$, $\boldsymbol{Q}(s) := \mathcal{L}[\boldsymbol{q}(t)]$, $\boldsymbol{G}_{\rm LP}(s) = \{\omega/(s+\omega)\}\boldsymbol{I}_3$ is the transfer function matrix of the first-order low-pass filter, ω is the cutoff frequency and $\boldsymbol{I}_3$ is the third-order identity matrix, respectively. If $\hat{\boldsymbol{\tau}}_{\rm dis}$ is close enough to $\boldsymbol{\tau}_{\rm dis}$, then a disturbance torque compensation $\boldsymbol{I}_a = \bar{\boldsymbol{K}}_t^{-1}\bar{\boldsymbol{M}}_d\boldsymbol{u} + \hat{\boldsymbol{\tau}}_{\rm dis}$ with $\boldsymbol{u} \in \mathbb{R}^3$ as new input yields a linearized and decoupled system $\ddot{\boldsymbol{q}} = \boldsymbol{u}$. Adopting a PD feedback control law, we can obtain a closed-loop system

$$\ddot{\boldsymbol{q}}(t) = \boldsymbol{K}_p(\boldsymbol{q}^d - \boldsymbol{q}(t)) + \boldsymbol{K}_v(\dot{\boldsymbol{q}}^d - \dot{\boldsymbol{q}}(t)), \cdots\cdots \quad (18)$$

where gain matrices $\boldsymbol{K}_p$ and $\boldsymbol{K}_v$ are positive definite diagonal. Using the PD control law with well-tuned gain matrices, the manipulator behaves along the desired trajectories.

In Eq. (18), the desired trajectories $\dot{\boldsymbol{q}}^d$ and $\boldsymbol{q}^d$ are calculated by Eqs. (6), (12) with $j = 4$, (14), (16), and the step-by-step integration of $\dot{\boldsymbol{q}}^d$. Using the PD control law with well-tuned gain matrices, the manipulator behaves according to the desired trajectories in consideration of the joint limits.

5.2 Experimental Setup and Results The three-DOF planar manipulator shown in Fig. 8 is used for experiment. This manipulator is controlled by a PC running a real-time Linux OS which is patched with Xenomai†. The control period is 1 ms. The rotating angle of each joint is obtained from an encoder attached to each DC motor via a counter board; Armature currents based on the control law (18) are interpolated to each DC motor by a D/A board through each DC servo driver. The physical parameters of the manipulator are same as in Sect. 4.

The experimental results are shown in Fig. 9. These figures show time responses of $\boldsymbol{q}$ and $\dot{\boldsymbol{q}}$. The experiments were carried out with initial condition:

$$\boldsymbol{q}(0) = (-5\,\text{deg},\ 90\,\text{deg},\ -45\,\text{deg}),\ \dot{\boldsymbol{q}}(0) = \boldsymbol{0}_3,$$
$$i.e.,\ \boldsymbol{r}(0) \simeq (0.25\,\text{m},\ 0.21\,\text{m}),\ \dot{\boldsymbol{r}}(0) = \boldsymbol{0}_2,$$

nominal parameters:

$$\bar{\boldsymbol{M}}_d = \text{diag}\{0.65\,\text{kg·m}^2,\ 0.25\,\text{kg·m}^2,\ 0.06\,\text{kg·m}^2\},$$

† Xenomai is a Free Software project in which engineers from a wide background collaborate to build a versatile real-time framework for the Linux platform. Available on http://xenomai.org/.

$$\bar{\boldsymbol{K}}_t = \text{diag}\{21\,\text{N·m/A},\ 17.64\,\text{N·m/A},\ 4.96\,\text{N·m/A}\},$$

tuning parameters $\omega = 150$ rad/s, $\boldsymbol{K}_p = \text{diag}\{144, 144, 144\}$, $\boldsymbol{K}_v = \text{diag}\{48, 48, 48\}$, $k_r = 0.01$ and $\rho = 0.1$. Figure 9 shows that tracking control to the desired trajectory generated by the proposed method can avoid the joint limits of the manipulator; the primary task was achieved with certain error, especially, in r_2. We can consider that this error occurred because the angular velocities changed steeply for avoiding the upper limit of q_2. Therefore, the simulation and experimental results validated the effectiveness of our proposed method while suggest necessity of extension to the dynamical level.

6. Conclusion

We have proposed an original PCF for avoiding joint limits of redundant manipulators. This function is based on a new concept, maximal admission of joint range of motion. The effectiveness of the proposed function was demonstrated numerically and experimentally through an example that a three-DOF planar manipulator performs a two-DOF end-effector task. The differences among the proposed and conventional functions were also discussed from the viewpoint of the definition and the simulation results.

In kinematic control of redundant robots, the proposed method can not only take physical limits into account but also utilize limited resources effectively, *e.g.*, it can move joints safely even in the close vicinity of the limit. The future works are to suppress steep variation of the desired velocities, to present a guideline on setting parameters (k_r, ρ), and so on. In particular, an extension of the proposed method into the dynamical level is necessary for improving the practical performance.

References

(1) A. Liégeois: "Automatic supervisory control of the configuration and behavior of multibody mechanisms", *IEEE Trans. Syst., Man, Cybern.*, Vol.SMC-7, No.12, pp.868–871 (1977)

(2) J. Rosen: "The gradient projection method for nonlinear programming. Part I. Linear constraints", *J. Soc. Ind. Appl. Math.*, Vol.8, No.1, pp.181–217 (1960)

(3) J. Baillieul: "Avoiding obstacles and resolving kinematic redundancy", Proc. IEEE ICRA, pp.1698–1704 (1986)

(4) Y. Nakamura, H. Hanafusa, and T. Yoshikawa: "Task-priority based redundancy control of robot manipulators", *Int. J. Robot. Res.*, Vol.6, No.2, pp.3–15 (1987)

(5) R.V. Mayorga and A.K.C. Wong: "A singularities avoidance approach for the optimal local path generation of redundant manipulators", Proc. IEEE ICRA, pp.49–54 (1988)

(6) D.N. Nenchev, Y. Tsumaki, and M. Takahashi: "Singularity consistent kinematic redundancy resolution for the S-R-S manipulator", Proc. IEEE/RSJ Int. Conf. IROS, pp.3607–3612 (2004)

(7) B.J. Nelson and P.K. Khosla: "Strategies for increasing the tracking region of an eye-in-hand system by singularity and joint limit avoidance", *Int. J. Robot. Res.*, Vol.14, No.3, pp.255–269 (1995)

(8) C.A. Klein and C.-H. Huang: "Review of pseudoinverse control for use with kinematically redundant manipulators", *IEEE Trans. Syst., Man, Cybern.*, Vol.SMC-13, No.3, pp.245–250 (1983)

(9) M.-J. Tsai: "Workspace geometric characterization and manipulability of industrial robots", Ph.D. dissertation, Dept. Mechanical Engineering, Ohio State Univ. (1986)

(10) H. Zghal, R.V. Dubey, and J.A. Euler: "Efficient gradient projection optimization for manipulators with multiple degrees of redundancy", Proc. IEEE ICRA, Vol.2, pp.1006–1011 (1990)

(11) T.F. Chan and R.V. Dubey: "A weighted least-norm solution based scheme for avoiding joint limits for redundant joint manipulators", *IEEE Trans. Robot. Autom.*, Vol.11, No.2, pp.286–292 (1995)

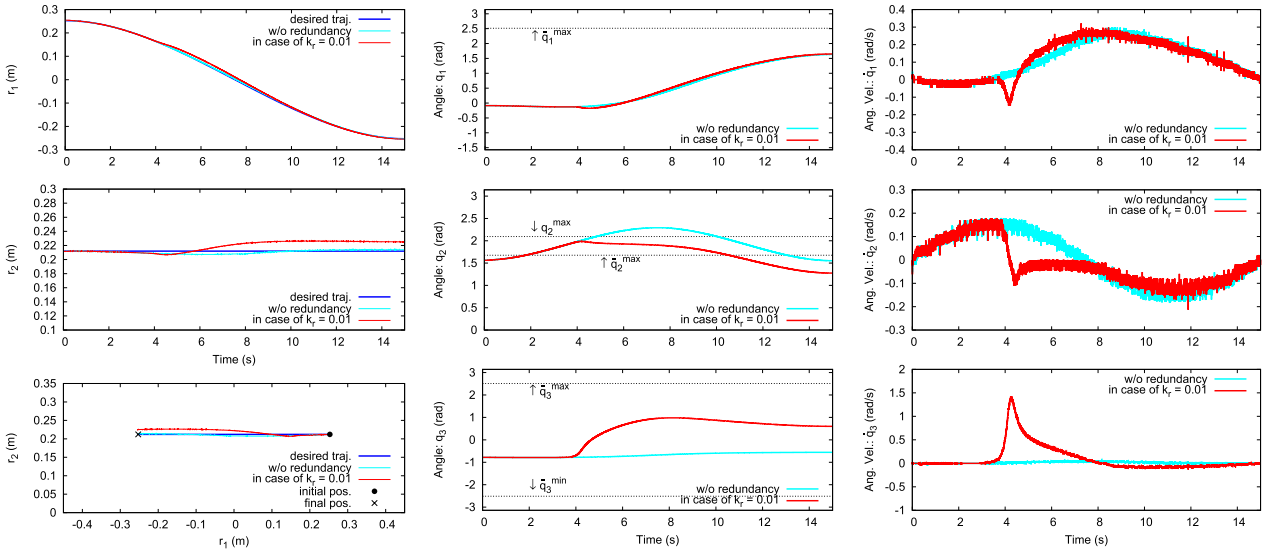

Fig. 9. Experimental results

(12) E. Marchand, F. Chaumette, and A. Rizzo: "Using the task function approach to avoid robot joint limits and kinematic singularities in visual servoing", Proc. IEEE/RSJ Int. Conf. IROS, Vol.3, pp.1083–1090 (1996)

(13) F. Chaumette and E. Marchand: "A redundancy-based iterative approach for avoiding joint limits: application to visual servoing", *IEEE Trans. Robot. Autom.*, Vol.17, No.5, pp.719–730 (2001)

(14) N. Mansard and F. Chaumette: "Directional redundancy for robot control", *IEEE Trans. Autom. Control*, Vol.54, No.6, pp.1179–1192 (2009)

(15) M. Marey and F. Chaumette: "A new large projection operator for the redundancy framework", Proc. IEEE ICRA, pp.3727–3732 (2010)

(16) M. Marey and F. Chaumette: "New strategies for avoiding robot joint limits: Application to visual servoing using a large projection operator", Proc. IEEE/RSJ Int. Conf. IROS, pp.6222–6227 (2010)

(17) T. Yoshikawa: "Manipulability and redundancy control of robotic mechanisms", Proc. IEEE ICRA, pp.1004–1009 (1985)

(18) J.M. Hollerbach and K.C. Suh: "Redundancy resolution of manipulators through torque optimization", *IEEE J. Robot. Autom.*, Vol.RA-3, No.4, pp.308–316 (1987)

(19) K.C. Suh and J.M. Hollerbach: "Local versus global torque optimization of redundant manipulators", Proc. IEEE ICRA, pp.619–624 (1987)

(20) N. Oda, T. Murakami, and K. Ohnishi: "Observer based local torque optimization in redundant manipulator", Proc. IEEE Int. Conf. IECON, Vol.2, pp.1915–1921 (1996)

(21) M. Ito, K. Kawatsu, and M. Shibata: "Maximal admission of joint range of motion based on redundancy resolution for kinematically redundant manipulators", Proc. SICE Annual Conf., pp.778–782 (2010)

(22) M. Ito, K. Kawatsu, and M. Shibata: "Maximal admission of joint range of motion based for kinematically redundant manipulators with joint limits", Proc. UKACC Int. Conf. Control, pp.489–494 (2010)

(23) M. Ito and M. Shibata: "Visual servo control admitting joint range of motion maximally", Lecture Notes in Control and Information Science (LNCIS), Vol.422, Springer-Verlag London, pp.225–235 (2012)

(24) M. Ito and M. Shibata: "Non-delayed visual servo control admitting joint range of motion maximally", *IEEJ Trans. IA*, Vol.132, No.5, pp.588–595 (2012) (in Japanese)

(25) F. Flacco, A. De Luca, and O. Khatib: "Control of redundant robots under hand joint constraints: Satruration in the null space", *IEEE Trans. Robotics*, Vol.31, No.3, pp.637–654 (2015)

(26) D. E. Whitney: "The mathematics of coordinated control of prosthetic arms and manipulators", *ASME J. Dyn. Syst., Meas., and Control*, Vol.94, No.4, pp.303–309 (1972)

(27) A. Atawnih, D. Papageorgiou, and Z. Doulgeri: "Kinematic control of redundant robots with guaranteed joint limit avoidance", *Robot. Auton. Syst.*, Vol.79, pp.122–131 (2016)

(28) C. P. Bechlioulis and G. A. Rovithakis: "Robust adaptive control of feedback linearizable MIMO nonlinear systems with prescribed performance", *IEEE Trans. Autom. Control*, Vol.53, No.9, pp.2090–2099 (2008)

(29) K. Ohnishi, M. Shibata, and T. Murakami: "Motion control for advanced mechatronics", *IEEE/ASME Trans. Mechatronics*, Vol.1, No.1, pp.56–67 (1996)

(30) B. R. Markiewicz: "Analysis of the computer torque drive method and comparison with conventional position servo for a computer-controlled manipulator", Technical Memorandum 33-601, Jet Propulsion Laboratory (1973)

Masahide Ito (Senior Member) was born in Aichi, Japan, on August 28, 1979. He received his B.S., M.S., and Ph.D. degrees in Information Science and Technology from Aichi Prefectural University, Japan, in 2002, 2004, and 2008, respectively. He was a Research Associate from 2007 to 2008, and an Assistant Professor from 2008 to 2013 in the Faculty of Science and Technology, Seikei University, Japan. In 2013, he joined Aichi Prefectural University, where he is currently a Lecturer of the School of Information Science and Technology. His research interests include vision-based control and nonlinear control for under- and fully-actuated robotic systems. He is a member of the IEEE, ISCIE, RoboCup Japanese National Committee, RSJ, and SICE.

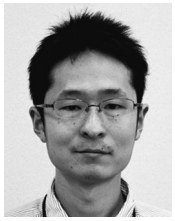

Kazuyoshi Kawatsu (Non-member) was born in Tokyo, Japan, on January 31, 1988. He received his B.E. degree in Science and Technology from Seikei University, Japan in 2010. He is currently with MITSUBISHI ELECTRIC BULIDING TECHNO-SERVICE CO., LTD., Shizuoka, Japan. His research interests include control of kinematically redundant manipulators.

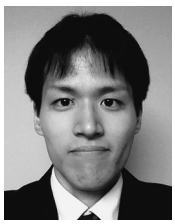

Masaaki Shibata (Senior Member) was born in Gunma, Japan, in 1968. He received his B.E., M.E., and Ph.D. degrees in Engineering from Keio University, Japan, in 1991, 1993, and 1996, respectively. From 1996 to 1998, he was with the MEIDENSHA CORPORATION. In 1998, he joined Seikei University, Japan, where he is currently a Professor of the Department of System Design Engineering. His research interests include robot vision and motion control for biped robots. He is a member of the IEEE, JSPE, and RSJ.